Diffusion−Viscosity Decoupling in Supercooled Aqueous Trehalose Solutions

ARTICLE *in* THE JOURNAL OF PHYSICAL CHEMISTRY B · OCTOBER 2008

Impact Factor: 3.3 · DOI: 10.1021/jp802806p · Source: PubMed

3 AUTHORS, INCLUDING:

Horacio R Corti
Comisión Nacional de Energía Atómica

119 PUBLICATIONS **1,462** CITATIONS

SEE PROFILE

Diffusion−Viscosity Decoupling in Supercooled Aqueous Trehalose Solutions

Horacio R. Corti,*,† Guillermo A. Frank,‡ and Mario C. Marconi‡,§

Departamento Física de Materia Condensada, Centro Atómico Constituyentes, Comisión Nacional de Energía Atómica, Av. General Paz 1499, 1650 San Martín, Argentina, Instituto de Química Física de Materiales, Ambiente y Energía (INQUIMAE), Facultad de Ciencias Exactas y Naturales, Universidad de Buenos Aires, Pabellón II, and Laboratorio de Electrónica Cuántica, Departamento de Física, Facultad de Ciencias Exactas y Naturales, Universidad de Buenos Aires, Pabellón I, Ciudad Universitaria, Buenos Aires, Argentina, and NSF ERC for Extreme Ultraviolet Science & Technology and Department of Electrical and Computer Engineering, Colorado State University, Fort Collins, Colorado 80525

Received: April 1, 2008; Revised Manuscript Received: July 6, 2008

The diffusional mobility of disodium fluorescein has been measured in supercooled aqueous solutions of trehalose, a widely used cryoprotectant disaccharide. The results were analyzed on the basis of the classical continuum hydrodynamic theory (Stokes−Einstein relationship) and compared with results for the diffusion and electrical conductivity of other ionic and nonionic solutes in trehalose and sucrose aqueous solutions. Disodium fluorescein obeys the classical model over a restricted range of inverse reduced temperatures, T_g/T, scaled by the glass transition temperature. Decoupling in neutral solutes takes place at higher values of T_g/T, while in ionic solutes it occurs all over the range of T_g/T studied, as observed for the water mobility in supercooled sugar solutions.

Introduction

Disaccharides, such as sucrose or trehalose, as other polyols are simple vitrifying agents which increase the glass transition temperature of water from 136 ± 1 K, as determined by Johari et al.[1] using DSC of hyperquenched glassy water, to values close to the ambient temperature. Their supercooled or glassy aqueous solutions are commonly used for the stabilization of biomolecules. In particular, aqueous solutions of trehalose have higher glass transition temperatures as compared to other sugar aqueous solutions, which prompted Green and Angell[2] to propose that this is the reason for its superior cryo- and anhydropreservation properties. Vitrification is not the only mechanism for stabilization of biomolecules or cells; the replacement of water hypothesis by Crowe et al.[3,4] suggests that trehalose could form hydrogen bonds with the polar groups of the lipids in biomembranes, replacing water of hydration at the membrane−fluid interface. Other hypotheses have been formulated, such as the water entrapment model by Belton and Gil[5] based on the thermodynamic data in solution by Arakawa and Timasheff[6] showing that sugars concentrate residual water molecules close to the biomolecule, the breaking of the hydrogen bond network of water by sugars proposed by Branca et al.,[7] or the reversible transformation of trehalose between two crystalline phases (anhydride and dihydrate) by Cesáro and co-workers.[8]

In this work we do not put emphasis on testing the abovementioned models, but we focus on the study of the diffusion of probes in aqueous sugar solutions close to the glass transition temperature. The dramatic increase in viscosity of these systems when cooled from room temperature to the supercooled region certainly should prevent the degradation of biomolecules by delaying their molecular mobility and, consequently, deterioration reactions. The prediction of the diffusion coefficients of solutes in supercooled aqueous solutions as a function of the temperature and composition is essential for modeling the cryopreservation process when the deterioration reactions are diffusionally controlled.

The simplest model to describe the diffusion of a spherical solute of hydrodynamic radius r_H in a continuum solvent having bulk viscosity η is the classical hydrodynamic model expressed by the Stokes−Einstein (SE) relation[9]

$$D = \frac{k_B T}{A \eta r_H} \tag{1}$$

where k_B is the Boltzmann constant, T the temperature, A a constant which depends on the type of friction on the solute surface (6π for the stick boundary condition and 4π for the slip boundary condition), and D the translational diffusion coefficient of the solute.

The diffusion of solutes in supercooled liquids presents a complex dynamic near the glass transition, where the bulk viscosity η is around 10^{12} Pa·s, and the SE relation (eq 1) is no longer valid because of a decoupling between D and η, which depends on the size relationship between the diffusing molecule and those of the surrounding medium[10,11] as well as on the type of interactions.[12] The breakdown of the SE relation below a crossover temperature close to $1.2T_g$ has been reported by Rössler and Sokolov,[13] Silescu and co-workers,[14,15] and Ediger and co-workers.[16,17]

There is little information on the decoupling of viscosity and diffusion in binary liquids, including aqueous mixtures, the most important systems from a practical point of view. Bordat et al.[18] analyzed the breakdown of the SE relation in a binary Lennard-Jones mixture by reverse nonequilibrium molecular dynamics (RNEMD). They concluded that below a temperature T_S (the onset of slow dynamics) the motion of particles is described by hopping between sites where particles are localized (cage

* Corresponding autor. E-mail: hrcorti@cnea.gov.ar. Phone: 5411 6772 7174. Fax: 5411 6772 7121

† Comisión Nacional de Energía Atómica and INQUIMAE, Universidad de Buenos Aires.

‡ Departamento de Física, Universidad de Buenos Aires.

§ Colorado State University.

10.1021/jp802806p CCC: $40.75
Published on Web 09/24/2008

effect) and the characteristic length of the single-particle positional fluctuation between these events is determined by the viscosity, while the characteristic size describe by the SE relation is approximately equal to the hydrodynamic radius of the particle. At high temperatures both lengths are identical and the SE relation holds.

Other models of the breakdown of the SE relation suggest the existence of dynamic heterogeneities.[10,11] A recent model of dynamical facilitation[19] predicts in general the breakdown of the SE relation in strong and fragile glass-forming liquids. However, it is not directly applicable to binary mixtures having the complexity of carbohydrate aqueous solutions.

Studies of the mobility of solutes in supercooled carbohydrate aqueous solutions are scarce. Champion et al.[20] observed the decoupling of the diffusion of fluorescein (a fluorescent probe) from the viscosity in sucrose−water mixtures by using the FRAP (fluorescence recovery after photobleaching) technique. Their results in the supercooled region extend close to the glass transition temperature of solutions with concentrations between 30% and 90% (w/w). The decoupling is observed for T_g/T above 0.86 and accounts for deviations up to more than 5-fold from the predictions in eq 1, and the temperature $T_c = T_g/0.86$ could be related to the critical temperature of the mode-coupling theory.[21]

Recently, Longinotti and Corti[22] studied the diffusion of ferrocenemethanol, a neutral solute, in sucrose aqueous solutions. The concentration of the sucrose solutions varied between 20 and 80 wt %, and the temperature was in the range of 5−25 °C, which corresponds to values of T_g/T between 0.48 and 0.87, covering the unsaturated and supercooled regions. It was observed that the diffusion−viscosity decoupling occurs at $T_g/T \approx 0.75$.

Magazù et al.[23] studied the diffusion of poly(ethylene oxide) and trehalose in aqueous solutions of trehalose using a photon correlation spectroscopy, a technique which yields self-diffusion coefficients in the very dilute limit. Therefore, only the measured diffusion coefficients of poly(ethylene oxide) in the temperature range of 20−85 °C and at concentrations of trehalose up to 18 wt % can be used to test the validity of the SE relation. Under these conditions the trehalose aqueous solutions are far from the supercooled regime, and as observed by the authors, the decoupling between diffusion and viscosity is not expected.

Lüdemann and co-workers[24] studied the intradiffusion coefficients of water (D_w) and carbohydrates (D_c) in aqueous solutions by the ^{13}C NMR technique. Their measurements in aqueous sucrose and trehalose include the supercooled region up to $T_g/T = 0.75$. At sugar concentrations higher than 50 wt % they observed a decoupling of D_s and D_w from the viscosity for both carbohydrates.

Similar results were observed for the decoupling of the electrical molar conductivity, Λ, and the viscosity of simple salts (NaCl, LiCl, $MgCl_2$) in aqueous solutions of trehalose and sucrose.[25−27] In that case the Walden law

$$\Lambda = \frac{z^2 F}{A\eta}\left(\frac{1}{r_+} + \frac{1}{r_-}\right) \tag{2}$$

where z is the ionic charge, r_+ and r_- are the ionic radii, A is the same constant as in eq 1, and F is the Faraday constant, is equivalent to the SE relationship for diffusion.

In this work we have measured the mobility of fluorescein in trehalose aqueous supercooled solutions using the FRAP technique (in its spot-bleaching version) to assess the range of validity of the classical hydrodynamic model in this important system and to estimate the deviation of the probe mobility from the SE relationship when the glass transition temperature is approached.

Experimental Section

The technique used for measuring the diffusion coefficient of fluorescein was FRAP. There are many ways to carry out the photobleaching technique. In this work spot-photobleaching was used, consisting of shining an intense beam to generate the photobleaching (*writing* beam) and a second much lower intensity beam with the purpose of exciting the fluorophore (*reading* beam). In the first stage a Gaussian-profile laser beam of wavelength $\lambda = 488$ nm, generated by an argon ion laser (Coherent Innova 90) of 700 mW equipment, was used. The sample was placed in the focal plane of a convergent lens in such a way as to obtain a cylinder-shaped volume lighting of radius between 12 and 16 μm. A sample thickness of 1 mm was used to avoid border effects. The details of the technique have been described elsewhere.[28]

The initial concentration of the fluorescent probe is c_0, and the concentration within the spot at the beginning of the recovery ($t = 0$), after a short bleaching time τ, is reduced to

$$c(r,0) = c_0 \exp[-k(r)\,\tau] \tag{3}$$

$k(r)$ being the first-order photobleaching rate constant. Under the experimental conditions it is reasonable to assume that the bleaching parameter $K = k(r)\,\tau$ in the exponent of eq 3 is given by[29] $K = \alpha\tau\, I(0)$, $I(0)$ being the beam intensity in the center of the spot, while the constant α depends on the physical properties of the fluorescent probe.

For a Gaussian reading beam with full width at half-maximum ω, the intensity is

$$I(r) = I(0)\exp\left(-\frac{2r^2}{\omega^2}\right) \tag{4}$$

The fluorescence response function, that is, the time evolution of the spatially averaged fluorescence due to the fluorescent probe molecules, is given by the expression derived by Axelrod et al.:[30]

$$F_G(t) = c_0 \nu K^{-\nu}\,\gamma(\nu, K) \tag{5}$$

where $\nu = (1 + 2t/\tau_D)^{-1}$, $\tau_D = \omega^2/4D$ (D being the diffusion coefficient of the fluorescent probe) is the characteristic diffusion time, and $\gamma(\nu,K)$ is the incomplete γ function. For the limit $K \rightarrow \infty$, eq 5 converges to

$$F_G(t) = c_0 \nu K^{-\nu}\,\Gamma(\nu) \tag{6}$$

where $\Gamma(\nu)$ is the γ function. For $K \geq 4$ and $t/\tau_D \geq 0.25$ the differences between both expressions are within 1%.[30]

An approximate expression for the spot-bleaching recovery function is obtained if it is assumed that the writing and reading beam widths are identical, although this is not always true. Moreover, the solution given by Axelrod et al.[30] is not linear in the parameter τ_D (or in the diffusion coefficient D), and this fact may introduce a significant error in its determination.

We have developed[28] an alternative expression for the fluorescence recovery function in the case of spot-bleaching which avoids the above-mentioned problems. Instead of considering a Gaussian writing beam and then assuming $K \rightarrow \infty$, we assume that the Gaussian writing beam is intense enough for bleaching uniformly a region of width ω'. Figure 1 shows the geometry of the diffusion problem for spot-bleaching in the case where the size of the writing beam ω' is smaller than the

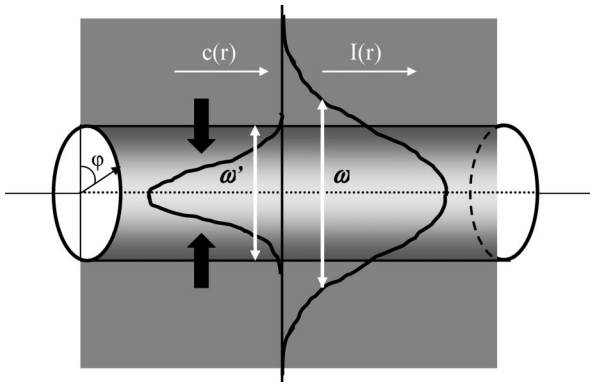

Figure 1. Representation of the bleached region (width ω'), the initial concentration profile $c(r,0)$ of the fluorescent probe, and the intensity profile $I(r)$ of the reading laser beam. The arrows indicate the radial diffusion of the unbleached probe molecules from outside the spot.

size of the reading beam ω. With this assumption the recovery function becomes

$$F(t) = c_0 \exp\left[-2\nu\left(\frac{\omega'}{\omega}\right)^2\right] \quad (7)$$

Neglecting the bleached molecules, the final concentration at long time should be equal to c_0. Equation 7 is linear in the diffusion coefficient and can be written in the form

$$Dt = -\frac{\omega^2}{4}\left[\left(\frac{\omega'}{\omega}\right)^2 \ln^{-1}\left(\frac{F(t)}{c_0}\right) + \frac{1}{2}\right] \quad (8)$$

The bleaching parameter K does not appear explicitly in eq 7, but the ratio ω'/ω, where ω' is the width of the bleached region, as indicated in Figure 1, contains information on the intensity of the probe photobleaching. The concentration profile of the bleached fluorescent probe, indicated in Figure 1, corresponds to a low value of the bleaching parameter K.

It was shown that the link between eqs 6 and 7 is given by the following relationship:[38]

$$\left(\frac{\omega'}{\omega}\right)^2 = a \ln K + b \quad (9)$$

valid for $K > 3$, where $a = 0.522$ and $b = 0.0748$.

The waist ω of the reading beam was obtained using as a reference system aqueous sucrose solutions with sucrose concentrations between 10 and 40.12 wt %. The diffusion coefficients of disodium fluorescein in sucrose solutions at 30 and 43.5 wt % are known, and the mean value of $\log(T/\eta D)$ is 14.83 ± 0.17 K Pa^{-1} m^{-2}.[20] Using eq 8, we obtained[28] the best value of the waist of the reading beam by fitting, $\omega = 70.1$ μm, which was used to obtain the diffusion coefficients of disodium fluorescein in trehalose−water mixtures.

The disodium fluorescein concentration in the trehalose−water mixtures is below 10 μM, the concentration of trehalose ranged from 27 to 80 wt %, and the temperature was varied between −15 and +20 °C. Thus, the ratio T_g/T changes between 0.55 and 0.95. The solutions with trehalose concentrations above 40 wt % and temperatures below 20 °C are supercooled and were prepared just before the experiment and kept at temperatures above the solubility curve to minimize the probability of crystallization. At the higher trehalose concentrations the measured fluorescence recovery curves extend over times close to 2500 s. However, as we will see later, the diffusion coefficients are estimated from the recovery curves at shorter times, usually below 600 s, in such a way that the crystallization of the sugar and convective effects can be neglected.

TABLE 1: Estimated Values of T_g for Trehalose Aqueous Solution

c (wt %)	T_g (K)	c (wt %)	T_g (K)
27.20	152.5	63.07	199.0
31.72	156.4	67.84	209.6
36.29	160.7	74.67	228.4
41.18	165.9	77.26	236.9
50.85	178.1	77.31	237.0
54.48	183.5	79.54	245.2
60.52	194.0	80.35	248.3

The analysis of the continuum hydrodynamic diffusion model requires knowledge of the dynamic viscosity of the sugar solutions. The calculation of η was performed using interpolation equations for the experimental results reported for aqueous solutions of trehalose by Miller et al.,[25,31,32] Magazú et al.,[7,23,33,34] Elias and Elias,[35] and Rampp et al.[24]

The Williams–Landel–Ferry (WLF) and power-law equations lead to differences between the calculated and the experimental values for trehalose solutions of up to 0.9 and 0.8 unit of log η, respectively. With the polynomial equation[36]

$$\log(\eta/\text{mPa}\cdot\text{s}) = 0.40 - 8.03(T_g/T) + 15.96(T_g/T)^2 \quad (10)$$

the viscosity of trehalose solutions could be fitted within a standard deviation of 0.10 unit of log η in the range $0.390 < T_g/T < 0.901$.

The values of T_g for the trehalose solutions were estimated from the experimental values (midpoint T_g) by Miller et al.[31,32] and Saleki-Gerhardt[37] using the Gordon and Taylor equation[38]

$$T_g = \frac{w_1 T_{g1} + w_2 k_{GT} T_{g2}}{w_1 + w_2 k_{GT}} \quad (11)$$

where w_1 and w_2 are the weight fractions of solute and water, respectively, $T_{g1} = 388$ K and $T_{g2} = 135$ K are the glass transition temperatures of pure sacharide and pure water, respectively, and $k_{GT} = 5.04 \pm 0.04$ is an adjustable parameter. Table 1 summarizes the values of T_g for the trehalose solutions at the concentrations studied in this work.

Results and Discussion

As mentioned above, the decoupling of the diffusion of fluorescein and the viscosity of the supercooled sucrose aqueous solutions was first observed by Champion et al.[20] using an interference fringe pattern FRAP technique, previously validated with the conventional concentration profile method.[39] The viscosity of the sucrose solution was fitted by Champion et al.[20] by resorting to the WLF equation over the whole range of temperature using their own viscosity data for $T - T_g \geq 60$ K and those by Bellows and King[40] in the range $30 \text{ K} \leq T - T_g \leq 130$ K. The fitted viscosity as a function of temperature shows that, in the low-temperature region, closer to the glass transition temperature, the WLF equation underestimates the experimental values by a factor larger than 10. For this reason, with the aim of comparing with our own measurements,[28] we redraw the Stokes−Einstein plot of these authors by using the viscosity fit similar to that used for trehalose solutions (eq 10), namely

$$\log(\eta/\text{mPa}\cdot\text{s}) = 2.82 - 17.11(T_g/T) + 24.68(T_g/T)^2 \quad (12)$$

The values of the viscosity of sucrose solutions used for the fit and the details of the procedure were reported elsewhere.[36] Equation 12 reproduces the experimental data with a standard deviation of 0.075 unit of log η in the range $0.405 < T_g/T < 0.893$.

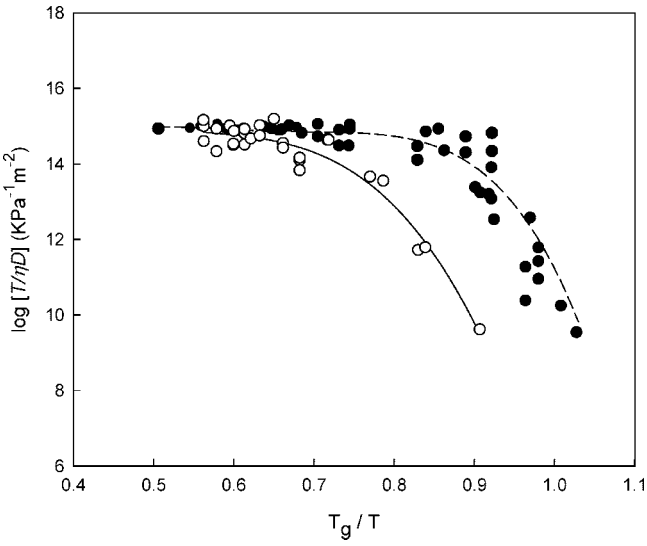

Figure 2. Stokes−Einstein plot ($T/\eta D$ vs T_g/T) for the diffusion of disodium fluorescein in aqueous sucrose. The closed symbols and dashed line correspond to the recalculated data by Champion et al.[20] The open symbols and full line correspond to the data by Corti et al.[28]

Figure 2 shows the recalculated values by Champion et al.[20] along with our results obtained using the alternative solution with the robust linear fit.[28]

The averaged hydrodynamic radius of disodium fluorescein in water, as determined by diffusion measurements using different techniques,[41−44] is around 0.51 and 0.76 nm for stick and slip conditions, respectively, in very good agreement with those found in diluted sucrose aqueous solutions[20] (0.49 ± 0.15 and 0.74 ± 0.22 nm for stick and slip conditions, respectively) in the region where the SE relation holds and also with the value reported by Mustafa et al.[44] for the diffusion of fluorescein in hydropropyl cellulose.

At higher values of the inverse reduced temperatures the diffusion−viscosity decoupling occurs for both sets of data. However, while our measurements indicate that the decoupling appears around $T_g/T \approx 0.65$, from the data by Champion et al.[20] the decoupling takes place at $T_g/T \approx 0.80$. The reason for this discrepancy is not clear, so the study of the diffusion of fluorescein in trehalose aqueous solutions could help clarify this point.

The recovery function, transformed according to eq 8, and the results for the recovery function given by eq 5 are shown in Figure 3 for disodium fluorescein in trehalose at two different concentrations. The main features of the fitting process were discussed elsewhere.[28]

It is clear that the robust linear fit of eq 8 for $F(t) < 0.9$ is better than the corresponding fit using the three-point method,[30] mainly because the robust linear fit emphasizes the data at intermediate time, where the experimental errors are minimized.

The results for the diffusion of the fluorescein in trehalose−water mixtures in the normal and supercooled regimes are summarized in Table 2. Only the diffusion coefficients obtained with the linear robust estimator (eq 8) are shown along with the viscosity of the corresponding solutions at the working temperatures. In general, the uncertainty of the diffusion coefficients obtained with the robust linear fit is much lower than that obtained using the three-point method, particularly for supercooled trehalose solutions.

From the values of the diffusion coefficients, reported at the same concentration and temperature, it is concluded that the deviation of the individual measurements from the mean value is higher than the standard deviation of the measurements. This is particularly true in the case of the supercooled trehalose solutions, that is, for all the solutions with trehalose concentrations higher than 40 wt %, as can be inferred from the supplemented phase diagram of the system trehalose−water shown in Figure 4, based on data by Miller et al.[31] Therefore, while the scatter of diffusion data in the stable solutions (trehalose concentrations lower than 40 wt %) is clearly a consequence of the experimental technique, the larger scatter for the supercooled solutions could be due to the onset of trehalose crystallization in the samples. In the supercooled regime, the formation of sugar embryos could make the system nanoheterogeneous and the water eviction from the matrix could take place before the crystallization of the sugar. The magnitude of this effect is dependent on the way the sample reached the supercooled regime and would affect the reproducibility of the diffusion measurements, although without having a notorious effect on the calculated glass transition temperature, which would only change when massive crystallization takes place.

The standard deviation of our measurements for trehalose supercooled solutions is similar to that observed in our measurements in aqueous supercooled sucrose solutions and smaller than those reported by Champion et al. in highly concentrated (supercooled) sucrose solutions.

In spite of the fact that the onset of crystallization strongly affects the reproducibility of the diffusion coefficient in the supercooled solutions, the results, when analyzed globally, allow us to obtain reliable conclusions on the decoupling phenomena in this system.

Thus, the SE plot in Figure 5 clearly shows that, for moderate concentration solutions at $T_g/T < 0.60$, the SE relation holds and the hydrodynamic radius of fluorescein is slightly lower than that determined in water and diluted aqueous sucrose solutions. Probably the interaction of fluorescein with sucrose leads to species having larger sizes than in the case of trehalose. Recent studies of the electrical conductivity of borate ions in sucrose and trehalose solutions[45] demonstrate that trehalose forms borate esters of smaller hydrodynamic sizes than those of sucrose, albeit in this case the solute forms covalent bonds with the saccharide.

Above $T_g/T \approx 0.60$ a diffusion−viscosity decoupling is observed. The diffusion of the solute is 3 orders of magnitude higher than that expected from the SE relationship at the highest value of T_g/T studied. By comparing the SE plots of Figures 2 and 5, it could be concluded that the decoupling for the diffusion of fluorescein in sucrose and trehalose solutions takes place at around the same T_g/T and its magnitude is also rather similar. This is indeed expected taking into account the structure of both disaccharides and considering that their interaction with fluorescein should not be too different.

The chemical structure and the charge of the fluorescein anion depend on the pH, as shown in Figure 6.[46] The angle between the plane of the xanthene moiety and the plane of the benzoate ring is 90° in the dianion form and 70° in the monoanion form.

We prepared the samples by adding sodium hydroxide to get pH ≈ 8, in such a way that the dianion species is predominant. The solvation of the fluorescein dianion in the water and water−sucrose mixtures in the low T_g/T region corresponds to solvation layers (assumed spherical) of thickness around 0.14 and 0.29 nm, respectively, depending on the boundary conditions adopted for the solute−solvent friction.[28] The results of this

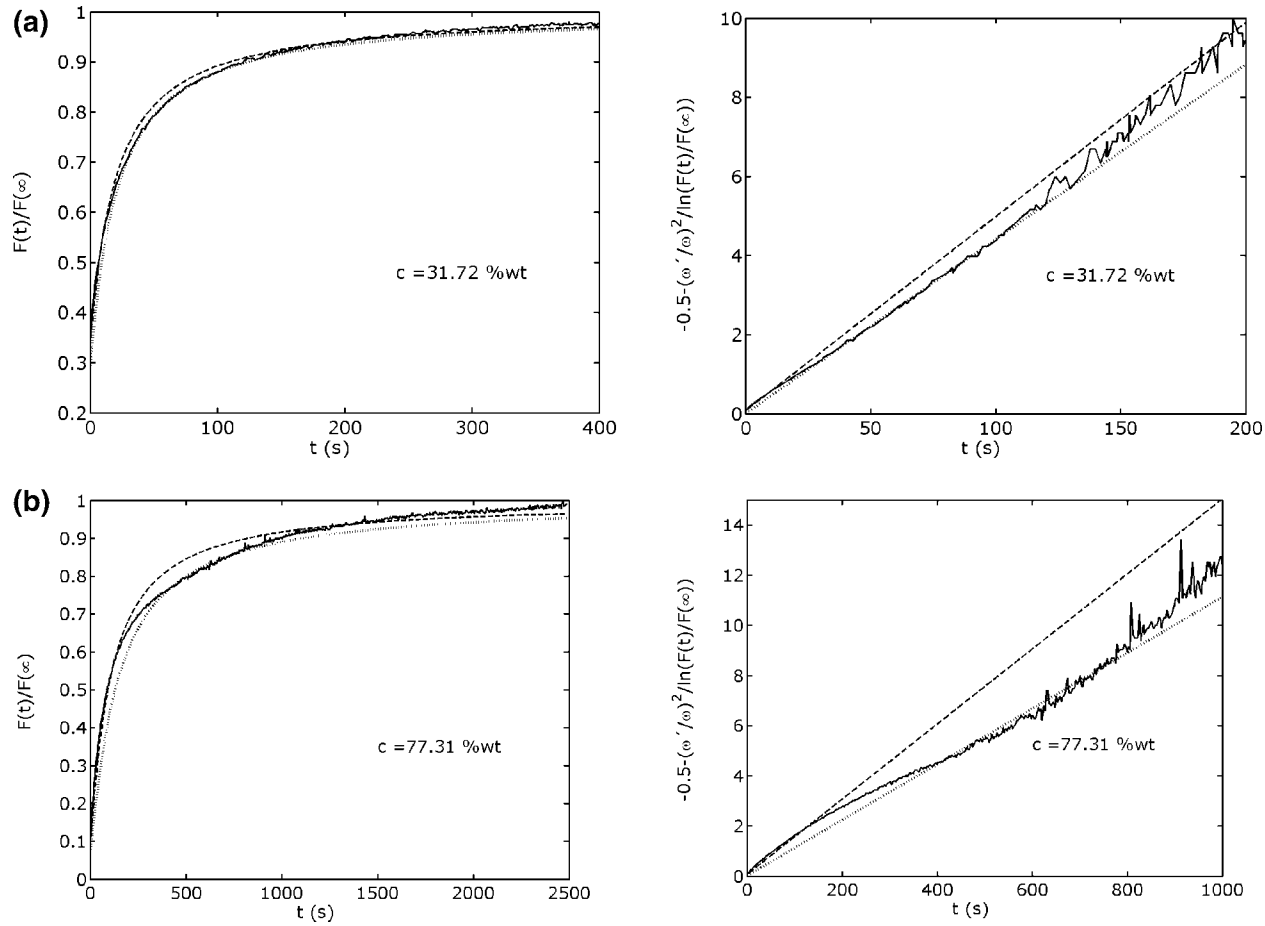

Figure 3. Recovery functions in their raw form (left) and represented according to the right-hand-side transformation of eq 8 (right) for the fluorescence of disodium fluorescein in trehalose aqueous solutions: (a) trehalose, 31.72 wt %; (b) trehalose, 77.31 wt %. The solid lines correspond to the experimental data, dashed lines to the Axelrod et al.[30] fitting method, and dotted lines to the robust fit.

work indicate that the solvation of the dianion in aqueous trehalose is similar to or even smaller than that in sucrose solutions.

In the high T_g/T region, where decoupling is observed, it is worth comparing the mobility of different solutes in supercooled trehalose and sucrose aqueous solutions. This can be accomplished by plotting the inverse of the effective hydrodynamic radii calculated from diffusion and electrical conductivity measurements by using eqs 1 and 2. It should be emphasized that the size parameters obtained are not real radii of the solutes because these equations assume a spherical solute and a continuum structureless solvent. Nevertheless, this size parameter gives us an idea of the solute hydrodynamic size when the classical hydrodynamic model holds and, when plotted against T_g/T, allows detection of a deviation from this regime, that is, diffusion−viscosity decoupling.

Figure 7 shows the inverse of the hydrodynamic radii of the electrolyte ($r_+^{-1} + r_-^{-1}$) in sucrose and trehalose aqueous solutions for NaCl and for electrolytes containing ions larger than a water molecule, as in the case of the tetrabutylammonium bromide and iodide. They were calculated from the measured electrical conductivity and viscosity using eq 2 with stick conditions. The results correspond to NaCl in sucrose aqueous solutions[26] at concentrations between 65.11 and 76.17 wt % and temperatures between −20 and +50 °C, NaCl in trehalose aqueous solutions[26] at 68.07 wt % and temperatures between −20 and +45 °C, tetrabutylammonium bromide in sucrose aqueous solution[27] at 76.27 wt % and temperatures between −15 and +35 °C, and tetrabutylammonium iodide in trehalose aqueous solution[27] at 39.13 wt % and temperatures between −5 and +20 °C. Also plotted are the values in pure water.

The behavior of NaCl and tetrabutylammonium salts in sucrose and trehalose aqueous solutions is similar: all of them exhibit a decoupling of the ion mobility and the viscosity which extends all over the range of T_g/T investigated. In fact, the inverse ionic hydrodynamic radius of these electrolytes increases monotonically with T_g/T, indicating that the SE relationship is not obeyed even in water or dilute solutions. The origin of the decoupling, as indicated by molecular dynamic simulations for the NaCl−trehalose−water systems,[25] is related to the existence of local heterogeneities, where ions are more likely surrounded by water than trehalose. The same mechanics could be operating for the bulky ions of the tetrabutylammonium salts.

In Figure 7 we plotted for comparison the inverse hydrodynamic radius of disodium fluorescein in trehalose aqueous solutions and in water, which is similar to that found for this fluorescent probe in sucrose solutions,[47] where diffusion−viscosity decoupling occurs at $T_g/T \approx 0.76$. Generally speaking, the behavior of this salt is similar to that found for NaCl and tetrabutylammonium iodide in aqueous trehalose, except that, within the experimental scatter characteristic of the FRAP measurements, the SE relationship holds in the narrow region $0.45 < T_g/T < 0.60$.

It should be noted that the hydrodynamic radius of the disodium fluorescein in a dilute sucrose aqueous solution from diffusion measurements[28] is 0.49 for stick conditions and 0.74 nm for slip conditions, while the crystallographic radius of the fluorescein dianion estimated using the method developed by

TABLE 2: Diffusion Coefficient of Fluorescein in Aqueous Solutions of Trehalose as a Function of the Concentration and Temperature

c (wt %)	T (K)	T_g/T	η (mPa·s)	K	D (10^{11} m^2·s^{-1})
27.20	295.8	0.5154	3.24	2.40	29.2 ± 4.7
				2.81	21.3 ± 2.3
				2.38	28.2 ± 3.5
31.72	295.8	0.5289	4.22	2.09	17.6 ± 1.2
				2.61	21.4 ± 3.2
				3.01	12.1 ± 0.9
				2.78	12.2 ± 1.0
				2.62	11.3 ± 0.7
36.29	295.4	0.5440	5.82	3.72	14.5 ± 1.3
				4.14	13.3 ± 1.4
				3.67	12.1 ± 1.4
				4.51	10.2 ± 1.0
41.18[a]	293.2	0.5657	9.39	3.91	9.6 ± 0.6
				4.09	3.7 ± 0.1
50.85[a]	295.0	0.6037	23.4	3.68	23.9 ± 1.6
	293.1	0.6076	25.8	4.37	17.9 ± 1.3
	288.0	0.6184	34.2	3.45	11.6 ± 0.5
54.48[a]	278.1	0.6600	109	2.97	2.84 ± 0.07
60.52[a]	295.4	0.6568	99.1	3.20	4.8 ± 0.1
63.07[a]	296.2	0.6720	156	2.68	5.9 ± 0.2
67.84[a]	283.3	0.7400	1.47×10^3	1.37	0.19 ± 0.02
74.67[a]	296.6	0.7700	4.47×10^3	1.18	1.92 ± 0.09
				1.17	1.09 ± 0.05
				1.41	0.751 ± 0.009
77.31[a]	294.3	0.8055	1.85×10^4	7.76	1.47 ± 0.04
				11.76	1.37 ± 0.01
79.54[a]	288.9	0.8486	1.21×10^5	1.67	0.44 ± 0.01
80.35[a]	291.2	0.8527	1.46×10^5	1.48	0.232 ± 0.006

[a] Supercooled solutions.

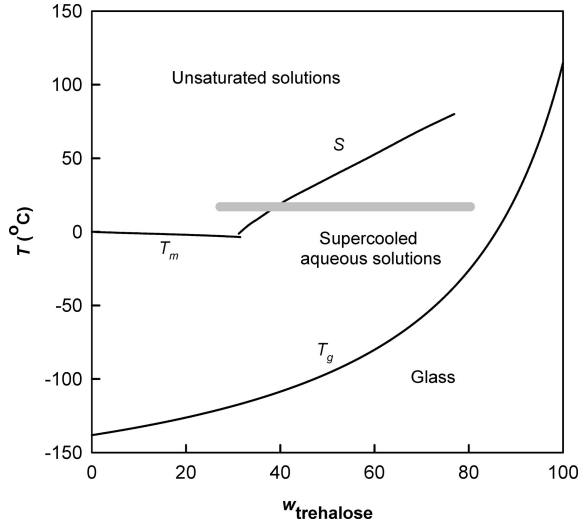

Figure 4. Supplemented phase diagram for trehalose aqueous solutions. T_m corresponds to the equilibrium water melting temperature, S to the trehalose solubility equilibrium curve,[31] and T_g to the trehalose glass transition temperature.[31] The gray area corresponds to the region where the diffusion measurements were performed.

Hubbard and Douglas[48] for oblate ellipsoids is $r_C \approx 0.35$ nm. Therefore, the smaller inverse hydrodynamic radius of disodium fluorescein in water and dilute solutions as compared to the other salts is due to a combination of the effect of the size and solvation of the fluorescein dianion.

The plateau in the SE plot for the disodium fluorescein recalls to us the behavior of ferrocenemethanol in sucrose aqueous solutions,[22] where the SE relation is obeyed up to $T_g/T \approx 0.75$. It seems reasonable to rationalize these results in terms of the interaction of these solutes with the water−disaccharide mixture.

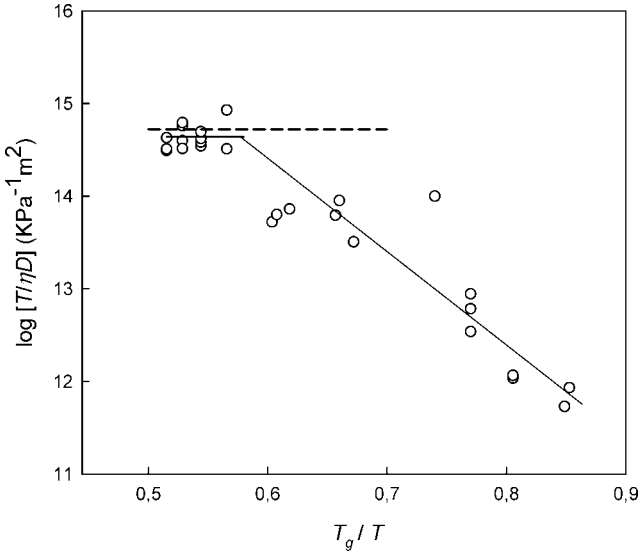

Figure 5. Stokes−Einstein plot ($T/\eta D$ vs T_g/T) for the diffusion of fluorescein in trehalose aqueous solutions. The dashed line represents the value for fluorescein in water. Full lines are only an aid to the eye (the horizontal line between $T_g/T = 0.51$ and $T_g/T = 0.57$ corresponds to the averaged value in this range).

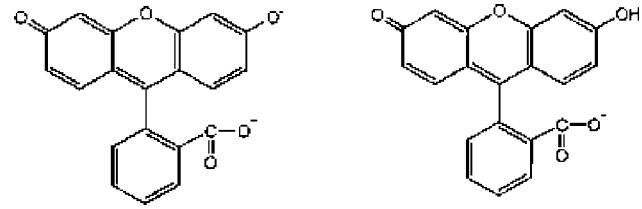

Figure 6. Chemical structure of the fluorescein dianion (left) and the carboxylate form of the monoanion (right).

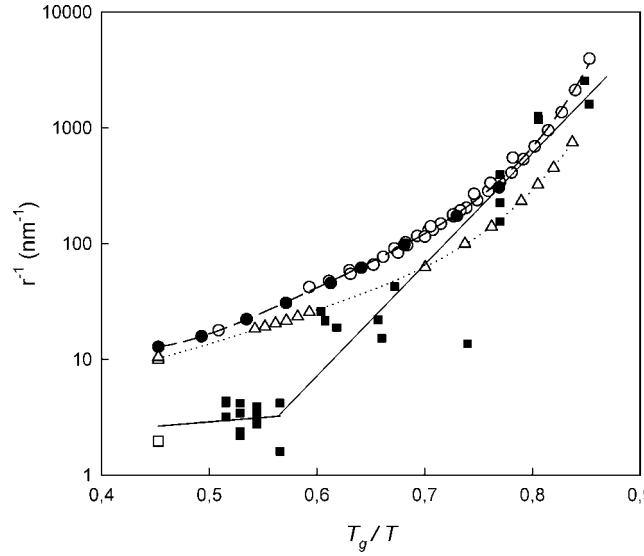

Figure 7. Inverse hydrodynamic radius of NaCl in sucrose (○) and trehalose (●) solutions, $(C_4H_9)_4NBr$ in sucrose (Δ) and trehalose (▲) solutions, calculated from the measured Walden product ($\Lambda\eta$),[26,27] and fluorescein calculated from the measured diffusion coefficient in aqueous trehalose (■) and water (□).

The diffusion of the disodium fluorescein in the FRAP experiment is dominated by the mobility of the bleached fluorescein dianion, with the sodium anions following the diffusion field created by the dianion diffusion. Both the fluorescein dianion and the neutral ferrocenemethanol are nonspherical solutes having a classical hydrodynamic mobility far from the glass

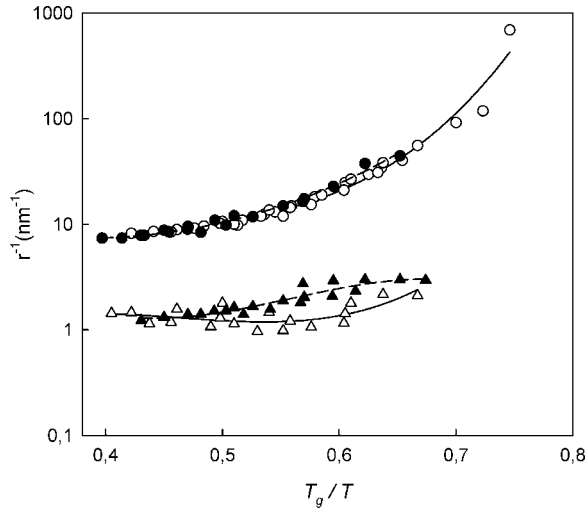

Figure 8. Inverse hydrodynamic radii for the diffusion of water (circles) and carbohydrate (triangles) in trehalose (open symbols, full line) and sucrose (closed symbols, dashed line) solutions calculated from diffusion data.[24]

transition temperature (low values of T_g/T). When the solution becomes deeply supercooled, the presence of dynamic heterogeneities and/or the onset of preferential solvation (structural heterogeneities) will induce the breakdown of the SE relationship.

To support this argument, it is interesting to compare the behavior of these solutes in the water−disaccharide mixtures with the results of the diffusion of the main components (water and disaccharide). The diffusion data by Lüdemann and co-workers[24] for the water−sucrose and water−trehalose systems are summarized in Figure 8, which shows how the intradiffusion coefficient changes with T_g/T. The range of T_g/T values plotted in Figure 8 corresponds to disaccharide concentrations between 30 and 70 wt % and temperatures from 25 to 80 °C.

Despite of the fact that the SE relationship is strictly valid at infinite dilution of the solute in the solvent and that the curves shown in Figure 8 could be affected by solute−solute interactions, the behavior of the diffusion coefficients of water in sucrose and trehalose solutions resembles that found for ionic solutes; that is, the decoupling is observed in the entire range of inverse reduced temperatures. On the other hand, the diffusion of the disaccharides seems to follow the SE relationship independently of the degree of supercooling.

The higher mobility of water molecules, as compared to the sugar ones, in the deep supercooled regime suggested by the diffusion measurements by Lüdemann and co-workers[24] is also supported by the coarse grain molecular dynamics simulations performed by Molinero et al.[49] for sucrose−water mixtures.

A theoretical model developed by Xia and Wolynes,[50] assuming a mosaic structure for a pure supercooled liquid with different solute mobilities, indicates that the deviation from the SE relation depends on the ratio between the size of the solute and the size of the solvent molecules, r/R, being negligible when $r/R > 6$, but increasing when $r/R \rightarrow 1$. Also, the deviation becomes larger when the glass transition temperature is approached. This would explain the larger deviation for NaCl and $(C_4H_9)_4NBr$ in sucrose and trehalose aqueous solutions as compared to fluorescein and also the deviation for the diffusion of water in water−sugar samples, not observed for the diffusion of the sugar (Figure 8). However, the model fails to account for the lower deviation of ferrocenemethanol compared to fluorescein observed in sucrose.[22,47] Thus, solute−solvent interactions could affect the mosaic structure of the supercooled solvent and should play an important role in determining the breakdown of the SE relationship.

The correlation between the diffusion of water and ions in these supercooled solutions could be a consequence of the fact that ions are moving in local water-rich environments in these systems[25] and consequently the ion and water flows could be coupled. The mosaic model of mobility in supercooled liquids, as applied to these water−sugar binary systems, should also include the possibility that regions of slow and rapid mobilities exist even far from the glass transition temperature as a consequence of structural nanoheterogeneites due to the different hydrogen bond connectivities of water and sugar.

Moreover, the presence of ionic solutes modifies, locally, the structure of the binary solution. Indeed, we expect that small ions solvate preferentially with water,[25] while in the case of large ions this trend could be reduced or even the sugar could replace water in the ion solvation layer. Thus, preferential solvation could enhance structural heterogeneities in these binary water−sugar solutions.

Large neutral solutes, such as as ferrocenemethanol, and highly nonspherical bulky ions, such as fluorescein dianion, obey the SE relationship unless dynamical heterogeneities induce decoupling when the glass transition temperature is approached. It is logical that this takes place at lower T_g/T for fluorescein than for ferrocenemethanol, taking into account that its ionic character could induce structural heterogeneities.

Conclusions

The decoupling of the diffusion and viscosity of disodium fluorescein was observed in supercooled aqueous solutions of trehalose. Similarly to previously reported results for this solute in aqueous sucrose solutions,[28] the SE relationship is not obeyed in a wide range of inverse reduced temperatures, $T_g/T > 0.6$.

The diffusion of small solutes in trehalose and sucrose at temperatures close to the glass transition temperature is much higher than that predicted using the Stokes−Einstein relationship. For $T_g/T \approx 0.85$ the diffusion coefficient of fluorescein is a factor of 1000 larger than that obtained by extrapolating the high-temperature value using the hydrodynamic model. Accordingly, the rate of diffusionally controlled deterioration reactions in aqueous systems close to the glass transition temperature could be several orders higher than predictions based on eq 1.

For ionic solutes, the decoupling between mobility and viscosity is related to the presence of not only dynamic heterogeneities as suggested by the mosaic model of supercooled liquids, but also structural heterogeneities in the water−sugar solutions enhanced by the presence of ions. Ionic solutes showing preferential solvation with water can diffuse more easily through these water-rich regions having lower local viscosities than the bulk viscosity.

The mobility of the bulky ionic disodium fluorescein is not directly coupled with the water mobility in the disaccharide−water mixture, and the SE relationship is obeyed over a restricted region at low values of T_g/T. The breakdown of the SE relationship takes places at higher values of T_g/T for neutral solutes, as observed in ferrocenemethanol.[22]

The correlation between ionic interactions and decoupling or SE breakdown is complex,[51] particularly in mixed solvents such as the sugar−water mixtures studied here. Therefore, a more comprehensive understanding of the dynamics in these systems would require more studies on a diverse type of solutes with variable sizes and potential interactions.

Acknowledgment. We thank the ANPCyT (Grant PICT 6-32916), Consejo Nacional de Investigaciones Científicas y Técnicas (Grant PID 5977), and University of Buenos Aires (Project UBACyT X-220) for financial support. H.R.C. is a member of the Consejo Nacional de Investigaciones Científicas y Técnicas (CONICET). G.A.F. thanks the ANPCyT and CONICET for fellowship support.

References and Notes

(1) Johari, G. P.; Hallbrucker, A.; Majer, E. *Nature* **1987**, *330*, 552–553.
(2) Green, J. L.; Angell, C. A. *J. Phys. Chem.* **1989**, *93*, 2880–2882.
(3) Crowe, J. H.; Leslie, B.; Crowe, L. M. *Cryobiology* **1994**, *31*, 355–366.
(4) Crowe, J. H.; Crowe, L. M.; Oliver, A. E.; Tsvetkova, N.; Wolkers, W.; Tablin, F. *Cryobiology* **2001**, *43*, 89–105.
(5) Belton, P. S.; Gil, A. M. *Biopolymers* **1994**, *34*, 957–961.
(6) Arakawa, T.; Timasheff, S. N. *Biochemistry* **1982**, *21*, 6536–6544.
(7) Branca, C.; Magazù, S.; Maisano, G.; Migliardo, P.; Villari, V.; Sokolov, A. P. *J. Phys.: Condens. Matter* **1999**, *11*, 3823–3832.
(8) Sussich, F.; Skopec, C.; Brady, J. W.; Cesáro, A. *Carbohydr. Res.* **2001**, *334*, 165–176.
(9) Bird, R. B.; Stewart, W. E.; Lighfoot, E. N. *Transport Phenomena*; John Wiley & Sons: New York, 1960.
(10) Chang, I.; Fujara, F.; Geil, B.; Heuberger, G.; Mangel, T.; Silescu, H. *J. Non-Cryst. Solids* **1994**, *248*, 172–174.
(11) Cicerone, M. T.; Blackburn, F. R.; Ediger, M. D. *J. Chem. Phys.* **1995**, *102*, 471–479.
(12) Le Meste, M.; Voilley, A. J. *J. Phys. Chem.* **1988**, *92*, 1612–1616.
(13) Rössler, E.; Sokolov, A. P. *Chem. Geol.* **1996**, *128*, 143–153.
(14) Ehlich, D.; Silescu, H. *Macromolecules* **1990**, *23*, 1600–1610.
(15) Heuberger, G.; Sillescu, H. *J. Phys. Chem.* **1996**, *100*, 15255–15260.
(16) Blackburn, F. R.; Cicerone, M. T.; Hietpas; G.; Wagner, P. A.; Ediger, M. D. *J. Non-Cryst. Solids* **1994**, *172*−*174*, 256–264.
(17) Ediger, M. D. *J. Non-Cryst. Solids* **1998**, *235*−*237*, 10–18.
(18) Bordat, P.; Affouard, F.; Descamps, M.; Müller-Plathe, F. *J. Phys.: Condens. Matter* **2003**, *15*, 5397–5407.
(19) Jung, Y.; Garrahan, J. P.; Chandler, D. *Phys. Rev. E* **2004**, *69*, 061205.
(20) Champion, D.; Hevert, H.; Blond, G.; Le Meste, M.; Simatos, D. *J. Phys. Chem. B* **1997**, *101*, 10674–10679.
(21) Rössler, E. *Phys. Rev. Lett.* **1990**, *65*, 1595–1598.
(22) Longinotti, M. P.; Corti, H. R. *Electrochem. Commun.* **2007**, *9*, 1444–1450.
(23) Magazù, S.; Maisano, G.; Migliardo, P.; Villari, V. *J. Chem. Phys.* **1999**, *111*, 9086–9092.
(24) Rampp, M.; Buttersack, C.; Lüdemann, H.-D. *Carbohydr. Res.* **2000**, *328*, 561–572.
(25) Miller, D. P.; Conrad, P. B.; Fucito, S.; de Pablo, J. J.; Corti, H. R. *J. Phys. Chem. B* **2000**, *104*, 10419–10425.
(26) Longinotti, M. P.; Mazzobre, M. F.; Buera, M. P.; Corti, H. R. *Phys. Chem. Chem. Phys.* **2002**, *4*, 533–540.
(27) Longinotti, M. P.; Corti, H. R. *Carbohydr. Res.* **2008**, *343*, 2650–2656.
(28) Frank, G. A.; Marconi, M. C.; Corti, H. R. *J. Solution Chem.* DOI 10.1007/510953-008-9330y.
(29) Eggeling, C.; Widengren, J.; Rigler, R.; Seidel, C. A. M. *Anal. Chem.* **1998**, *70*, 2651–2659.
(30) Axelrod, D.; Koppel, D. E.; Schlessinger, J.; Elson, E.; Webb, W. W. *Biophys. J.* **1976**, *16*, 1055–1069.
(31) Miller, D. P.; de Pablo, J. J.; Corti, H. R. *Pharm. Res.* **1997**, *14*, 578–590.
(32) Miller, D. P.; de Pablo, J. J.; Corti, H. R. *J. Phys. Chem. B* **1999**, *103*, 10243–10249.
(33) Magazú, S.; Maisano, G.; Migliardo, P.; Middendorf, H. D.; Villari, V. *J. Chem. Phys.* **1998**, *109*, 1170–1174.
(34) Branca, C.; Magazú, S.; Maisano, G.; Migliardo, P.; Migliardo, P.; Romeo, G. *J. Phys. Chem. B* **2001**, *105*, 10140–10145.
(35) Elias, M. E.; Elias, A. M. *J. Mol. Liq.* **1999**, *83*, 303–310.
(36) Longinotti, M. P.; Corti, H. R. *J. Phys. Chem. Ref. Data* **2008**, *37*, 1503–1575.
(37) Saleki-Gerhardt, A. Ph.D. Thesis, University of Wisconsin, Madison, 1993.
(38) Gordon, J. M.; Taylor, J. S. *Appl. Chem.* **1952**, *2*, 493–500.
(39) Champion, D.; Hevert, H.; Blond, G.; Simatos, M. D. *J. Agric. Food Chem.* **1995**, *43*, 2887–2891.
(40) Bellows, R. J.; King, C. J. *AIChE Symp. Ser.* **1973**, *69*, 33–41.
(41) Moore, A. W.; Jorgenson, J. W. *Anal. Chem.* **1993**, *65*, 3550–3560.
(42) Mustafa, M. B.; Tipton, D. L.; Russo, P. S. *Macromolecules* **1989**, *22*, 1500–1504.
(43) Mosier, B. P.; Molho, J. J.; Santiago, J. G. *Exp. Fluids* **2002**, *33*, 545–554.
(44) Mustafa, M. B.; Tipton, D. L.; Barkley, M. D.; Russo, P. S.; Blum, F. D. *Macromolecules* **1993**, *26*, 370–378.
(45) Longinotti, M. P.; Corti, H. R. *J. Solution Chem.* **2004**, *33*, 1029–1038.
(46) Wang, L.; Roitberg, A.; Meuse, C.; Gaigalas, A. K. *Spectrochim. Acta, Part A* **2001**, *51*, 1781–1791.
(47) Corti, H. R.; Frank, G. A.; Marconi, M. C. *J. Solution Chem.* DOI 10.1007/510953-008-9329-4.
(48) Hubbard, J. B.; Douglas, J. F. *Phys. Rev. E* **1993**, *47*, R2983−R2986.
(49) Molinero, V.; Çağin, T.; Goddard, W. A., III. *Chem. Phys. Lett.* **2003**, *377*, 469–474.
(50) Xia, X.; Wolynes, P. G. *J. Phys. Chem. B* **2001**, *105*, 6570–6573.
(51) Hall, R. W.; Wolynes, P. G. *J. Phys. Chem. B* **2008**, *112*, 301–312.

JP802806P